

Conjugated Polymer (MEH-PPV:MWCNTs) Organic Nanocomposite for Photodetector Application

Isam M. Ibrahim¹

Abeer H. Khalid^{2*}

Received 19/2/2018, Accepted 2/10/2018, Published 9/12/2018



This work is licensed under a [Creative Commons Attribution 4.0 International License](https://creativecommons.org/licenses/by/4.0/).

Abstract:

Fabrication of a photodetector consists of the conjugated polymer "MEH-PPV"- poly (2-methoxy-5-(2'-ethylhexyloxy)-1,4-phenylenevinylene) and MEH-PPV:MWCNT nanocomposite thin film. The volume ratio investigated was 0.75:0.25. MEH-PPV was dissolved in chloroform solvent and doped with MWCNTs. The spin coating method was used to achieve a facile and low cost photodetector. The absorption spectrum decreases by adding the CNTs. The PL spectrum detected recombination curve results by doping the polymer with CNTs, and AFM measurement showed an increase of roughness average from (0.168 to 2.43nm) of "MEH-PPV" and "MEH-PPV:CNTs", respectively. The doping ratio 0.25, which has a higher photoresponsivity, was evaluated at 1.70 A/W and 2.14 A/W of the UV and Vis. wavelength range. Time-dependent photocurrent analysis showed that the higher sensitivity was 176.56 % at 350nm and 290.99% at 500 nm of the "MEH-PPV:MWCNTs" thin films, while I-V characteristics showed a rectifying behavior.

Keywords: Organic photodetector, Nanocomposite Photodetector, Photodetector

Introduction:

In the last few decades, photo detectors have been extensively studied in various fields such as biomedical imaging, night vision and optical communications because of their potential applications(1–5). Low-cost applications of organic material solar cells and photodetectors have garnered attention in a wide area (6-8), along with the fabrication of organic devices using low-cost methods based on evaporation or printing and coating on different substrates (9). These include not only traditional substrates for electronics like glass or silicon but also metal foils and polymers (10). The combination of organic photodiodes with micro- and nanostructures is promising, as the steps necessary for production to manufacture these devices is easy. The organic photodiode is a nanotechnology research object itself since the device operation depends on a nanocomposite system such as a conjugated polymer and a functionalized fullerene(11-13). Organic molecules with π - conjugated structures accommodate a variety of new materials with metallic and semiconducting properties (14). A conjugated system consists of alternation between single and double bonds.

The fundamental property in a conjugated system is π -electrons which are more mobile than σ -electrons. Thus, the π -electrons can move by hopping from position to position. These π -electrons permit light absorption such as in (solar cells) and light emission such as in (OLEDs). The Highest Occupied Molecular Orbital "HOMO" and Lowest Unoccupied Molecular Orbital "LUMO" correspond to the molecular (π - π^*) orbital (15). MEH-PPV is defined as (poly (2-methoxy-5-(2'-ethylhexyloxy)-1,4-phenylenevinylene)), the common usage of organic polymer is due to the sensitivity of its photo physics and polymer group to rigid state morphology (16). Also, MEH-PPV is known as electron donor (17) and perfectly excite generators in optoelectronic application (18). Comparatively, it is characterized as having low conductivity because of low hole and electron mobility in contrast to inorganic semiconductor material (17). "MEH-PPV" is organic conjugated polymer; it is known as an incoming material that collects optical and electronic properties (19). The development of nanomaterial that is based on carbon nanotube and detection of carbon nanotube have piqued the interest of researchers (20). The unique properties of carbon nanotube attracts a attention in many applications such as electronic structures (21) and, biological systems (22). The composites of carbon nanotubes with conducting polymers were used in different applications in the

¹Department of Physics, College of Science, University of Baghdad, Baghdad, Iraq.

²Ministry of Science and Technology, Laser and Optoelectronic Center, Baghdad, Iraq

*Corresponding author: odourflower25@yahoo.com

past such as polymer light emitting diodes PLED (23, 24), sensors (25), and photovoltaic cells (26). The extended and comprehensive applications of carbon nanotube with polymer composites have perhaps led to those in the scientific community to consider CNTs a part of the polymer family (27). The previous studies were concerned with photodetection., Dhinesh B. V. et . al., fabricated mechanically flexible 2D organic-inorganic hybrid thin film photodetectors that consist of inorganic MoS_2 and organic g-C 3N_4 nanosheets for broadband photodetection with ratios (5:5 hybrid films) which exhibited excellent photodetection performance in terms of ON/OFF photocurrent ratio, specific detectivity, responsivity, and response time with both 365 and 532nm illumination (28). Xiaopeng Guo et. al., fabricated an organic-inorganic hybrid UV photovoltaic detector with a large responsivity of $40\text{mA}\cdot\text{W}^{-1}$ in an Al/PFO/Zno/ITO structure. This study paves the way for developing large-array, high-performance, high-uniformity, light-weight and low-cost UV FPA detectors(29).

Materials and Methods:

Preparation of Multi Wall Carbon Nanotube (MWCNT) and MEH-PPV solutions:

The black powder (MWCNT) was first weighted at 10mg and dissolved in 10ml of (N,N-dimethylformamide DMF) as a solvent to obtain the concentration of 1mg/ml. The solution was placed in a magnetic stirrer for 6 hours and then sonicated for 8 hours to obtain a homogeneous solution, and was then diluted to the concentration of 0.01mg/ml of MWCNT.

The concentration of the polymer MEH-PPV, Sigma-Aldrich, $M_n=(40.000-70.000)\text{g/mol}$, was prepared by weighting 10mg and dissolving in 10ml of chloroform (CHCl_3) as a solvent, to obtain the concentration of 1mg/ml. Next, the "MEH-PPV" solution was doped with MWCNT solution and sonicated to enable these solutions to mix well with a volume ratio (0.75:0.25) of "MEH-PPV:MWCNTs" nanocomposite solution. The MEH-PPV:MWCNTs nanocomposite solution was deposited on Si substrate (111) using the spin coating method at 1500 rpm for 1 minute, then dried at 100°C to remove any residual solvent. Finally, electrical contact made from aluminum metal was deposited on the top of the film using the thermal evaporation technique. A spin coating system (ACE 200) was used in this study, surface of the thin films was carried out using an Atomic Force Microscope (SPM, Model AA3000), tip NSC35/AIBS from Angstrom Advanced Inc (USA), while UV-Vis measurements were conducted using an (OPTIMA SP-3000 UV-VIS spectrophotometer)

with a wavelength range from 190-1100nm. PL measurement was done using an Agilent Tech. Fluorescence spectrophotometer. The SPECTROFLUOROMETER DETECTOR (RF-551) ver. 2.3A programmable and scanning' was used, to measure the responsivity of the photodetector with the range of incident wavelengths(200-900nm), by using a FIUKE, 8846A -6-1/2 DIGIT precision multimeter. I-V characteristics are measured in a forward and reverse bias circuit using a DIGITAL PICOAMMETER (Model:DPM-111). Fig. 1 shows the structure of photodetector device. To calculate the spectral responsivity of the tested detector (i.e., the responsivity as a function of wavelength), the photocurrent density generated from the tested detector is simply divided by the calculated power density as shown in the following equation:

$$R(\lambda) = J_{ph}(\lambda) / P_{in}(\lambda) \dots \dots \dots (1)$$

where $J_{ph}(\lambda)$ is the photocurrent density from the tested detector and $P_{in}(\lambda)$ is the incident power density measured with the photodetectors as a function of wavelength(30).

$$S = (I_{ph} - I_d / I_d) * 100\% \dots \dots \dots (2)$$

where S is the sensitivity, I_{ph} is the photocurrent and I_d is the dark current which can be calculated from the tested detector (31). In this work, we demonstrated that the conductive polymer and nanocomposite materials of MEH-PPV:MWCNT enhance the responsivity of the emission spectrum by adding CNTs as a photodetector device .

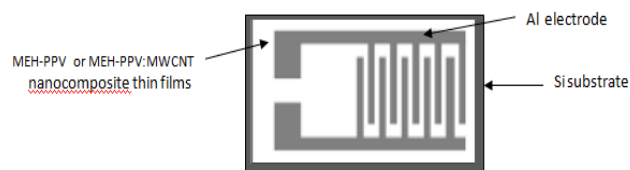


Figure1. Structure of the photodetector device

Results and Discussion:

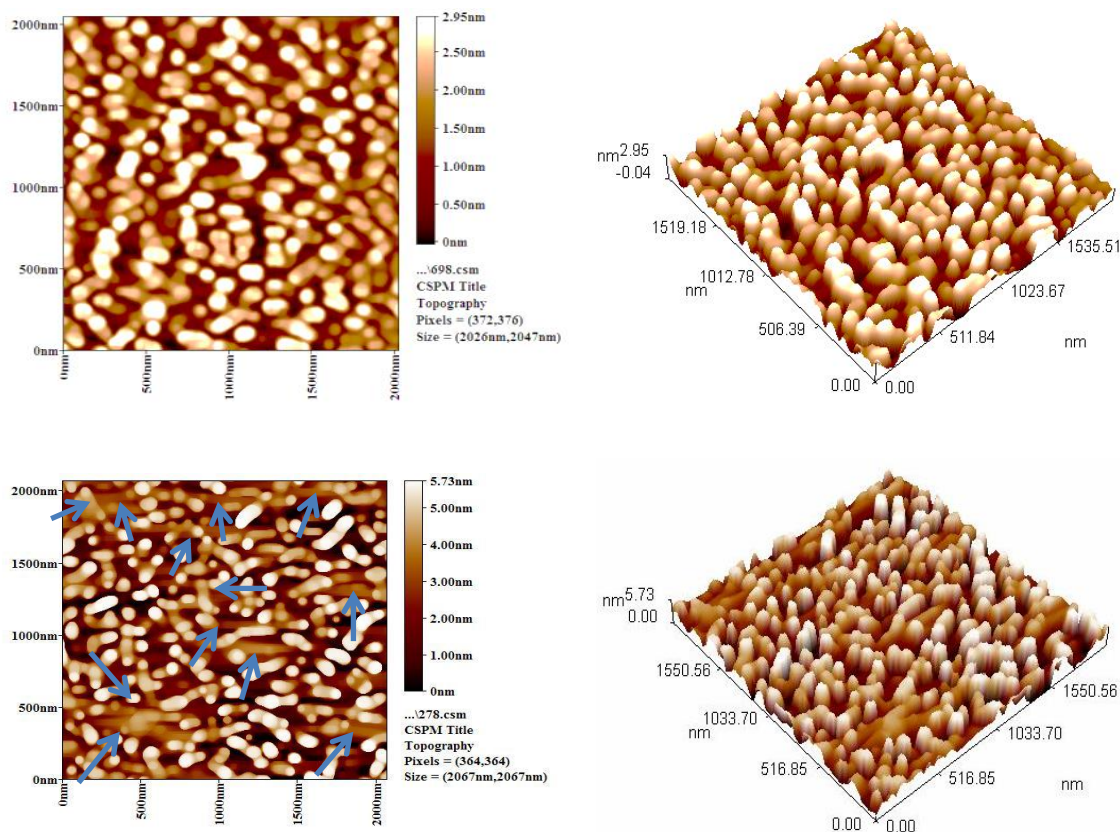
Structural Properties

The morphology of dispersion CNTs in an organic polymer as a nanocomposite material was investigated by analyzing the surface morphology, using AFM images obtained in the tapping mode on area approximately $(2.05 \times 2.05) \mu\text{m}^2$, as shown in Fig 2. For the pure "MEH-PPV" and "MEH-PPV:MWCNT" a volume ratio of 0.75:0.25 was used for thin films.

Figure 2a illustrates (2D) and (3D) images of surface morphologies, and the dispersion of the polymer grain is uniform; this is due to the deposition method of choice: 1500 rpm spin coating speed and a suitable evaporating solvent, Fig 2b-(2D) image. The dispersion of CNT can be observed, which is indicated by the blue color arrows and these arrows illustrate the position of CNTs in 3D images, CNTs act as a filler resort to

fill the matrix of the polymer. MWCNT bundles can be observed as shadow bundles, which show that the organic polymer has wrapped around the bundles of carbon nanotube. This cross grid of interconnected carbon nanotube; could create an efficient charge transport between the interconnected conductive paths of MWCNTs and a high optical transperance level due to its evolution

structure (32). The average roughness of "MEH-PPV" (pure) and "MEH-PPV:MWCNT" thin films is 0.168, 2.43nm , respectively. The increase of the surface roughness is due to the formation of aggregation of the carbon nanotube within the polymer. The morphology study offers a mighty dependence on the carbon nanotube in the polymer matrix.



(b)

Figure 2. AFM images (tapping mode) 2D (left) and 3D (right) of "MEH-PPV" and "MEH-PPV:MWCNT" nanocomposite,(a) "MEH-PPV" (pure), (b) "MEH-PPV:MWCNTs"

Optical Characterization

A bsorption spectra of the organic polymer "MEH-PPV" and "MEH-PPV" doping with CNT nanocomposite thin films were carried out as shown in Fig 3. Two peaks have been shown in both spectra ranging from (300-375)nm for B-Band and (375-620)nm for Q-Band. The spectrum of the

polymer decreased by adding the CNT. This indicates that CNTs incorporate into the MEH-PPV matrix without modifying the chemical structure of the polymer and it is likely that molecular orbital hybridization between the HOMO of MEH-PPV and LUMO of MWCNTs is achieved and this result agrees with (14,33).

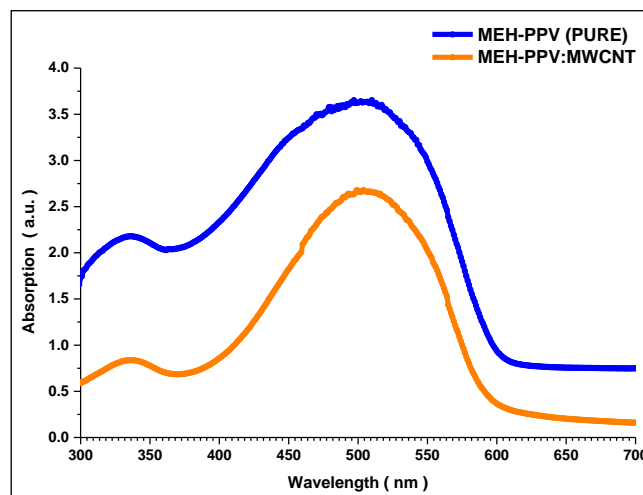


Figure 3. Absorption spectra of "MEH-PPV" (pure) and "MEH-PPV:MWCNT".

Figure 4 demonstrates the photoluminescence spectra of the organic polymer "MEH-PPV" and "MEH-PPV:MWCNT" nanocomposite: the photoluminescence peaks were in the range of (530-800)nm and excited by the wavelength 300nm. In the result there is no quenching spectrum but the PL intensity of the MEH-PPV:MWCNT nanocomposite increases in contrast to the pristine polymer "MEH-PPV", this may be due to the probability of the occurrence of recombination which will create an electron-hole pair. This is useful in an OLED application, and our result agrees with (34). The PL quenching process occurs through charging separation growing from the organic polymer to the carbon nanotube, photoinduction that happened through electron transfer causing an exciton dissociation at the interface between the polymer-carbon nanotube (35). The charge transfer process from polymer, which is considered a donor to the MWCNT, which is itself considered as an acceptor, is still occurring until the absorption process of light, dissociation, and charges causes separation at the interface of the polymer-carbon nanotube (36). The red shift is observed which is around 8.98nm of MEH-PPV:MWCNT nanocomposite. This may be due to the variation of effective organic conjugation length in addition to the carbon nanotube (37);, the energy gap reinforces the red shift and is calculated using the Eq. $E_g = 1240/\lambda$ decrease by doping the pristine polymer from 2.066 eV to 2.036eV.

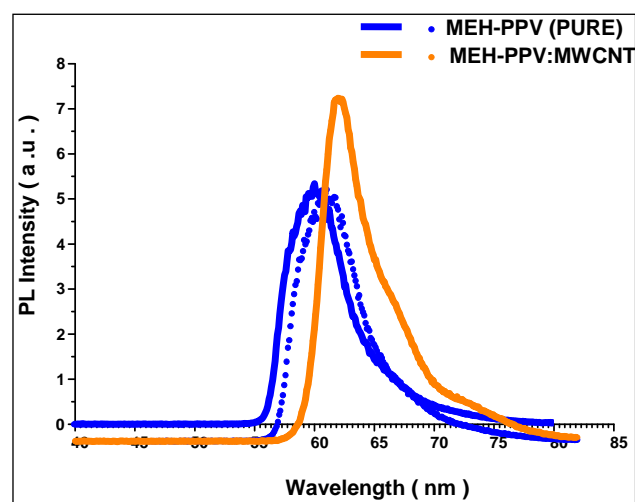


Figure 4. photoluminescence spectra of MEH-PPV and MEH-PPV:MWCNT at $\lambda_{exc}=300\text{nm}$

Electrical properties

Figure 5a shows the responsivity of organic MEH-PPV and nanocomposited MEH-PPV:MWCNT. The active common wavelengths of both spectra are in the range between (250-425)nm and (425-550)nm. The generated photocurrent showed a noticeable wavelength dependence, after illumination with wavelength excitations in the range of (200- 900)nm. The results indicate that the photocurrent gradually increases when doping the polymer with MWCNTs. The responsivity value that was calculated using Eq.(1) increased by adding CNTs from 0.82 A/W to 1.70 A/W of the wavelength range (250-425)nm and increased from 0.91 A/W to 2.14 A/W of the wavelength range (425-550)nm. The nature of the charges' transfer depends on the optical properties for both organic polymer and carbon nanotube as well as surface properties of the nanotube (38). AFM measurement supports the dispersion of CNT on the surface, regardless that CNT is homogeneously distributed.

The rate of the responsivity increased according to the photocurrent, this was due to high electrical conductivity of the carbon nanotubes. Thus, the resistance of the organic polymer reduced after doping the CNTs. Moreover, the polymer that is considered the (donor) is regulated by incorporation with CNTs considered as the (acceptor). The nanocomposite exciton photogenerated in the polymer under lighting conditions, and then diffused to interface between the acceptor and donor, the charge transport of the hole carrier from donor to the positive electrode and the electron

from acceptor to the negative electrode and then the total charge carrier stream through the external circuit and created electricity (39). For the time-dependent photocurrents, the sensitivity was measured of the selective wavelengths 350 and 500nm, and the values obtained were 19.23% and, 32.41%, of MEH-PPV (pure) respectively, and 176.56%, 290.99% of MEH-PPV:MWCNT nanocomposite photodetector respectively, as shown in Fig (5b-e). From these Figures, one can observe square pulses which refer to the fast response at these light wavelengths.

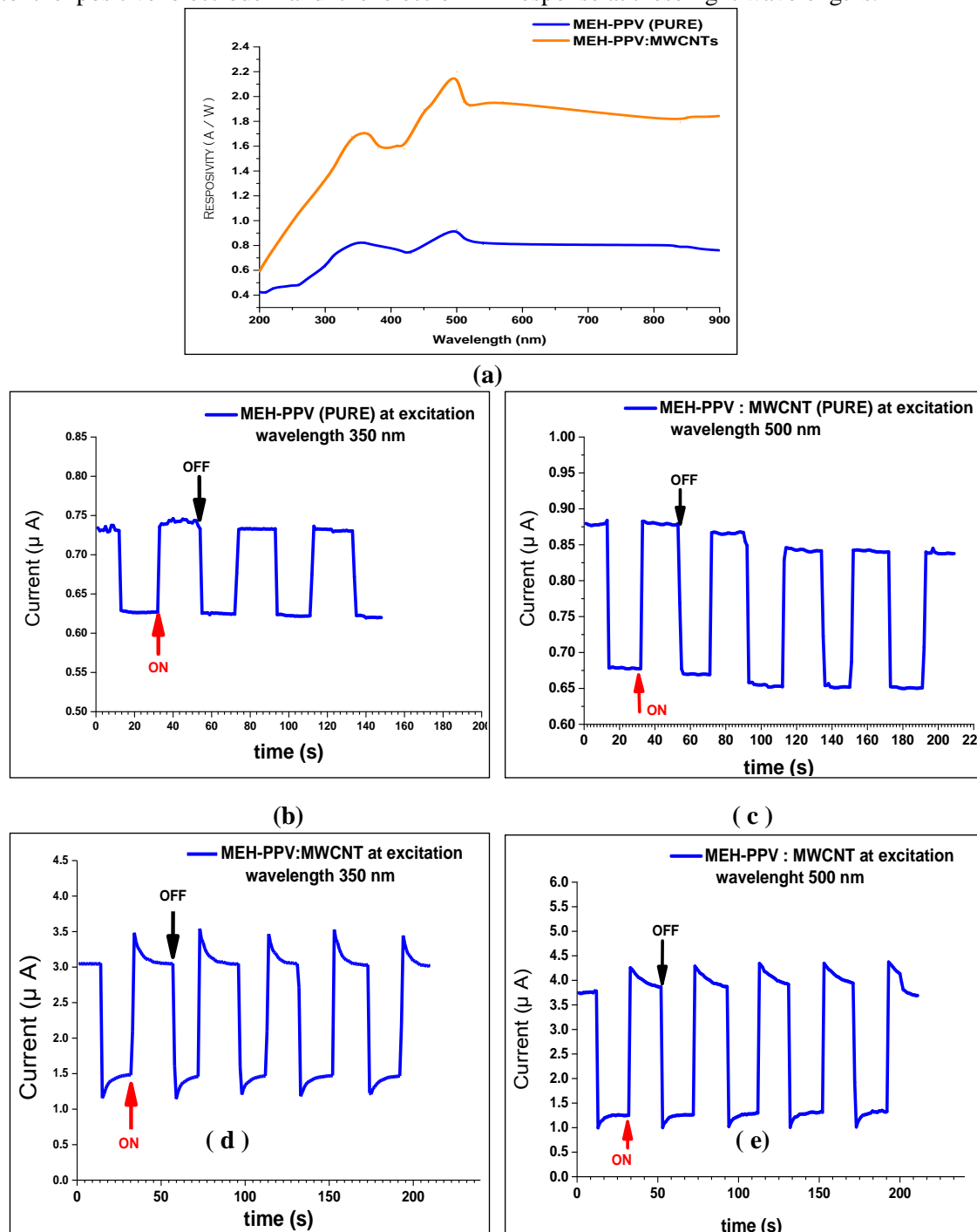


Figure 5. The spectral responsivity (a) and the time-dependent photocurrent of the MEH-PPV (pure) photodetector under (b) λ_{ex} . 350 nm, (c) λ_{ex} . 500 nm, and MEH-PPV:MWCNT photodetector (d) λ_{ex} . 350 nm, (e) λ_{ex} . 500 nm

Figure 6 show the I-V characteristics of MEH-PPV (pure) and MEH-PPV:MWCNT nanocomposite in both dark and illuminated condition with a halogen lamp. We can observe the Al metal contact and organic semiconductor form Schottky contact. In dark conditions the weak voltage observed in the reverse bias current and exponential increase in the forward bias current are the characteristic properties of rectifying contacts of the MEH-PPV and MEH-PPV:MWCNT, as shown

in Table 1. In illuminated conditions, the current exponential increased in the forward bias current approximately 100 times more than the pure polymer in the case of MEH-PPV:MWCNT, while the current exponential increased in the reverse bias current approximately 400 times more than the pure polymer of MEH-PPV:MWCNT. This is due to the CNTs as a network contact, dissociation exciton center, and charge transport channel.

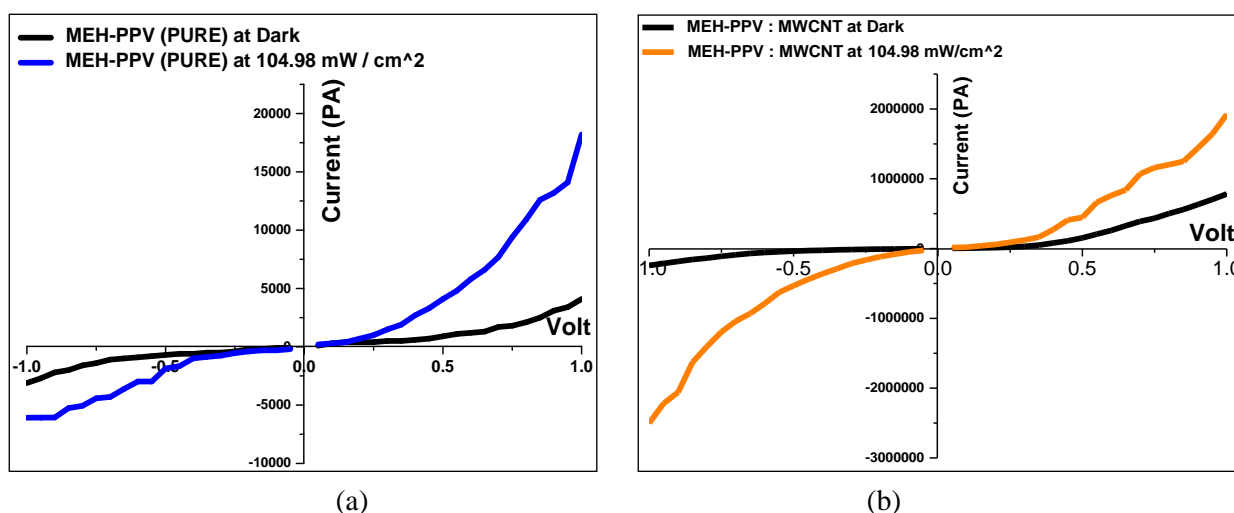


Figure 6. Current voltage (I-V) characteristic of (a) MEH-PPV (pure), (b) MEH-PPV:MWCNT under dark and illuminated condition

Table 1. the I-V curves position of "MEH-PPV" and "MEH-PPV:MWCNT"

Types state		I-V curve point position of MEH-PPV (pure)	I-V curve point position of MEH-PPV : MWCNT
Dark case	forward bias	(1,4100)	(1,782000)
	reverse bias	(-1,-3100)	(-1,-242000)
Illumination case	forward bias	(1,18200)	(1,1922000)
	reverse bias	(-1,-6080)	(-1,-2500000)

Conclusion:

Organic MEH-PPV and MEH-PPV:MWCNT nanocomposite photodetectors were successfully demonstrated in this study. Using the spin coating process and the fabricated device showed excellent rectifying characteristics in both dark and illuminated conditions, and the photoresponsivity increased when the polymer was doped with MWCNTs at the 0.25 ratio, while the sensitivity increased from 19.23% to 176.56% at 350nm and from 32.41% to 290.99% at 500nm. The enhancement of photocurrent in the UV and visible region is attributed to the dispersion MWCNT as a filler, dissociated charge center and transport charge channel, owing to their corresponding light

absorption region and thus to the generation of charge carriers. This suggests that a MEH-PPV:CNT nanocomposite photodetector is useful for both UV and visible light detections.

Conflicts of Interest: None.

Reference:

1. Fernando S, Eva SB, Pere C, Tajahuerce E, Jesús L. High-resolution adaptive imaging with a single photodiode. *Sci Rep.* 2015Sep18;5(14300):1-9.
2. Guo Z, Park S, Yoon J, Shin I. Recent progress in the development of near-infrared fluorescent probes for bioimaging applications. *Chem Soc Rev.* 2014Jan7; 43(1):16–29.
3. Gusarova NI, Koshchavtsev NF, Popov SV. Advantages of solid-state photodetectors for a spectral interval of 1.4–1.7 μm in night-vision devices. *Commun Technol Electron.* 2016Oct; 61(10):1211–1214.
4. Letian D, Yang MY, Jingbi Y, Ziruo H, Wei HC, Gang L, et al. Solution-processed hybrid perovskite photodetectors with high detectivity. *Nat Commun.* 2014 Nov20;5(5404):1-6.
5. Poomagal CT, Athappan M. Wireless Optical Communication for Underwater Applications. *IJARECE.* 2014Mar;3(3):312–315.
6. Shruti S, Kamlesh KJ, Ashutosh S. Solar Cells: In Research and Applications—A Review. *Mater Sci Appl.* 2015Dec24;6(12):1145-1155.

7. Huda AA, Zeid AA, Joseph GS, Saikh MW. Use of Carbon Nanotubes (CNTs) with Polymers in Solar Cells. *Molecules*. 2014Oct28;19(11): 17329-17344.
8. Hyunsoo K, Kyu-TL, Chumin Z, Jay GL, Jerzy K. Top illuminated organic photodetectors with dielectric/metal/dielectric transparent anode. *Org Electron*. 2015Feb08;20:103-111.
9. Karzazi Y. Organic Light Emitting Diodes: Devices and applications. *Mater Environ. Sci*. 2014;5(1):1-12.
10. Aliaksandr VZ, Darren JL. Processes for non-destructive transfer of graphene: widening the bottleneck for industrial scale production. *Nanoscale*. 2015Jun14;7(22): 9963–9969.
11. Mikkel J, Kion N, Frederik CK. Stability/degradation of polymer solar cells. *Sol Mat*. 2008 Jul; 92(7): 686-714.
12. Ulf G, Julian H, Boris R, Sebastian G, Uli L, Martina G. Large-scale patterning of indium tin oxide electrodes for guided mode extraction from organic light-emitting diodes. *Appl Phys*. 2008Nov12; 104(9):093111.
13. Stroisch M, Woggon T, Lemmer U, Bastian G, Violakis G, Pissadakis S. Organic semiconductor distributed feedback laser fabricated by direct laser interference ablation. *Opt Exp*. 2007Apr 2;15(7): 3968-3973.
14. Paez BA, Marulandab DM. Luminescence Tuning of MEH-PPV for Organic Electronic Applications. *Acta Phys Pol A*. 2016;129(6):1187-1190.
15. Tobias S. Top-Emitting OLEDs: Improvement of the Light Extraction Efficiency and Optimization of Microcavity Effects for White Emission. Dresden: Technics University;2014.
16. Anto RI, Hsiang CC, Wunshain F, Ying-SH, Jeng US, Hsu CH, et al. Structure and charge transport properties in MEHPPV. *Synth Met*. 2003Oct09;139(3):581-584.
17. Satish P, Qianxi L, Filippo M, Miyong J, Zuhua Z, Chen Z, et al. Dopant-configurable polymeric materials for electrically switchable devices. *Mater Chem*. 2006 Sep07;16(42):4160–4164.
18. Yong JC, Hyung HP, Stephen G, David CJ. A study on the incorporation of ZnO nanoparticles into MEH-PPV based organicoorganic hybrid solar cells. *Ceram Int*. 2012 Jan;38(1):S525-S528.
19. Hairong Z, Xuefang L, Yi L, Aic XZ, Guoqiang Y. Conformational transition of poly[2-methoxy-5-(2'-ethylhexoxy)-p-phenylene vinylene] in solutions: solvent-induced emitter change. *J Photochem Photobiol A Chem*. 2002Feb28;147(1):15-23.
20. Horacio JS, Ana MD, Eduardo L, Soledad V, Mari´an AG. Chemical sensors based on polymer composites with carbon nanotubes and graphene: the role of the polymer. *J Mater Chem A*. 2014Jun16;2(35):-14289-14328.
21. Endo M, Strano MS, Ajayan PM. Potential applications of carbon nanotubes. *Carbon Nanotubes*. 2008;111:13-62.
22. Sinbad S, Deborah Be, Superb M, Andrew JT, Eugenia VJ, Teresa DT. Multi-walled carbon nanotube length as a critical determinant of bioreactivity with primary human pulmonary alveolar cells. *Carbon*. 2014Nov01;78:26-37.
23. Tze BS, Ning L. Emerging Transparent Conducting Electrodes for Organic Light Emitting Diodes. *Electronics*. 2014Mar21;3(1):190-204.
24. Shengwei S, Silva SR. high luminance organic light emitting diodes with efficient multi walled carbon nanotube hole. *Carbon*. 2012 Sep;50(11): 4163-4170.
25. Ajeet K, Rajesh K, Sunil KA, Madhavan N, Malhotra BD, Shekhar B. Organic-Inorganic Hybrid Nanocomposite-Based Gas Sensors for Environmental Monitoring. *Chem Rev*. 2015May1;115(11):4571–4606.
26. Ruchuan L. Hybrid Organic/Inorganic Nanocomposites for Photovoltaic Cells. *Materials*. 2014Apr02;7(4):2747-2771.
27. Micah JG, Natnael B, Matteo P, Wade A. Nanotubes as polymers. *Polymer* 2009Oct09;50 (21): 4979–4997.
28. Dhinesh BV, Md. AH, Manas RP, Fan Z, Tom W, Omar FM, et al. 2D Organic-Inorganic Hybrid Thin Films for Flexible UV-Visible Photodetectors. *Adv Funct Mater*. 2017Feb13;27(15):1605554
29. Xiaopeng G, Libin T, Jinzhong X, Rongbin J, Kai Z, Sin KL, et al. Solution processable organic/inorganic hybrid ultraviolet photovoltaic detector. *AIP ADVANCES*. 2016May18;6(5): 055318.
30. Jia L. Photonic Devices. Cambridge University Press: Cambridge; 2005.
31. Lalchand AP, Ajinkya B, Mahendra DS, Vinita VD, Amalnerkar DP. Synthesis of ZnO nanocrystalline powder from ultrasonic atomization technique, characterization, and its application in gas sensing. *IEEE Sens J*. 2011Apr;11(4):939-946.
32. Walid A, Saidi H, Abdelaziz B. Comparative Study of Deposit through a Membrane and Spin-Coated MWCNT as a Flexible Anode for Optoelectronic Applications. *Nanomaterials*. 2016Mar;2016(45):7 pages.
33. Nadia C, Olfa D, Adnen L, Ali F, Abdelaziz B. Charge Transfer Properties in MEH-PPV/PS:MWCNTs Nanocomposites. *J Surf Eng Mater Adv Technol*. 2012Jan28;2(3):174-181.
34. Sarah MS, Zahid FS, Zulkifli Z, Noor UM, Rusop M. Aromatic and Non-Aromatic Solvent in Nanocomposited MEH-PPV:CNTs Thin Film for Organic Solar Cells. *IEEE-ICSE*. 2012 Sep10.
35. Kyu WL, Lee SP, Choi H, Kyu HM, Jae WJ, H. Kweon, et al. Enhanced electroluminescence in polymer-nanotube composites. *Appl Phys Lett*. 2007Jun;91(2):023110-0231103.
36. Qian L, Zunfeng L, Xiaoyan Z, Liying Y, Nan Z, Guiling P, et al. Polymer Photovoltaic Cells Based on Solution-Processable Graphene and P3HT. *Adv Funct Mater*. 2009Mar24;19(6): 894-904.
37. Vincenzo L, Nan Y. Molecular Mechanics of Binding in Carbon Nanotubes-Polymer Composites. *Materials Research*. 2000Dec;15(12): 2770- 2779.
38. Cuong TT, Matthew RP, Thien PN. Blue shift in the luminescence spectra of MEH-PPV films containing ZnO nanoparticles. *J Lumin*. 2008Dec;128(12):2031-2034.
39. Jenny N. Organic photovoltaic films. *Curr Opin Solid State Mater Sci*. 2002Feb;6(1): 87-95.

المركب النانوي العضوي للبوليمر المترافق MEH-PPV المدمج مع الانابيب الكربونية متعددة الجدران لتطبيقات الكاشف الضوئي

عبير حازم خالد²

عصام محمد ابراهيم¹

*جامعة بغداد، كلية العلوم، قسم الفيزياء، بغداد، العراق.
**وزارة العلوم والتكنولوجيا، مركز الليزر والكهرو بصريات، بغداد، العراق.

الخلاصة:

لقد تم التحقيق من تصنيع كاشف ضوئي يتكون الغشاء الرقيق من البوليمر المترافق poly(2-methoxy-5-(2'-ethylhexyloxy)-1,4-phenylenevinylene) و MEH-PPV:MWCNT و بنسبة حجمية 0.75 للبوليمر: 0.25 للكربون متعدد الانابيب. اذيب البوليمر المترافق MEH-PPV بمذيب الكلوروفورم وطعم بالانابيب الكربونية متعددة الجدران. طريقة الطلاء البرمي استخدمت للوصول الى كاشف ضوئي سهل وسعره منخفض. طيف الامتصاص ينخفض مع اضافة الكربون نانو تيوب. طيف الاستثنائية PL يكشف منحنى اعادة الاتحاد ينتج من تطعيم البوليمر مع الكربون نانو تيوب وقياسات مجهر القوة الذرية AFM يظهر زيادة بمعدل خشونة السطح من 0.168 الى 2.43 للبوليمر المترافق MEH-PPV: CNT و MEH-PPV: CNT بالتتابع. نسبة التطعيم 0.25 لها أعلى استجابة ضوئية وتقدر 1.70A/W و 2.14A/W لمدى الاطوال الموجية الفوق بنفسجي والمدى المرئي. تحليل التيار الضوئي المعتمد على الزمن يظهر بان التحسسية الاعلى كانت 176.56% عند الطول الموجي 350nm و 290.99% عند الطول الموجي 500 nm للاغشية الرقيقة MEH-PPV:MWCNTs، خصائص I-V تظهر سلوك المقوم.

الكلمات المفتاحية: الكاشف الضوئي العضوي، الكاشف الضوئي للمركب النانوي، الكاشف الضوئي